Kinetics of $A+B\rightarrow 0$ with driven diffusive motion

I. Ispolatov, P. L. Krapivsky, and S. Redner
Center for Polymer Studies and Department of Physics, Boston University, Boston, Massachusetts 02215
(Received 10 April 1995)

We study the kinetics of two-species annihilation $A+B\rightarrow 0$ when all particles undergo strictly biased motion in the same direction and with an excluded volume repulsion between same species particles. It was recently shown that the density in this system decays as $t^{-1/3}$, compared to $t^{-1/4}$ density decay in $A+B\rightarrow 0$ with isotropic diffusion and either with or without the hard-core repulsion. We suggest a relatively simple explanation for this $t^{-1/3}$ decay based on the Burgers equation. Related properties associated with the asymptotic distribution of reactants can also be acounted for within this Burgers equation description.

PACS number(s): 02.50.−r, 05.40.+j, 82.20.Wt

I. INTRODUCTION

While the kinetics of two-species annihilation $A+B\rightarrow 0$ has been extensively investigated and reasonably well understood [1–5], surprising results have been recently obtained in one dimension when both species move according to driven diffusive motion [6]. In this model, each particle can attempt a move only to the right and the attempt is successful only if the particle lands on an unoccupied site. If the particle lands on a site already occupied by a member of the same species, the move attempt is rejected and the initial particle remains at its starting position. However, if the particle lands on a site that is occupied by a member of the opposite species, then an $A+B\rightarrow 0$ reaction occurs and both particles disappear. This motion of each species may be viewed as strongly biased diffusion with a hard-core repulsion between same species particles.

For this system, one might naively anticipate that, by performing a Galilean transformation to a zero momentum reference frame, the long-time kinetics should be the same as that of $A+B\rightarrow 0$ with isotropic diffusion. For this latter system, the density is known to decay in time as $t^{-1/4}$ when the initial densities of the two species are equal [1–5]. This result has been found to hold both for the case of free diffusion and when an excluded-volume repulsion between same-species particles exists. In fact, such a Galilean universality has been derived for the case of single-species reactions and a special type of two-species reaction [7].

However, extensive numerical simulations in one dimension indicate, rather surprisingly, that for two-species annihilation with driven motion, the density asymptotically decays as $t^{-1/3}$ for a Poissonian initial distribution of the two species [6]. It was also found that the approach of the density to the $t^{-1/3}$ asymptotic form was rather slow. Even after 10^6 time steps, local estimates of the density decay exponent were still varying systematically with time. On the other hand, for isotropic diffusion, stable estimates of the decay exponent are achieved after 10^3–10^4 time steps. As we discuss below, there is an interesting reason for this slow approach to asymptotic behavior in the driven system.

In this paper we provide a theoretical argument for the $t^{-1/3}$ decay of the density in $A+B\rightarrow 0$ with driven diffusive motion. Our approach is based on first elucidating the dynamics of a single AB interface when the two species are initially separated (Sec. II). A continuum description in terms of the inviscid Burgers equation, together with continuity of particle currents, shows that the velocity of the interface can be determined in terms of the relative densities of the two adjoining species. This information is used to infer that when the initial condition is homogeneous and random, a typical single-species domain grows as $t^{2/3}$. This result, together with the fact that the density inside a domain is simply related to initial density fluctuations, leads to the $t^{-1/3}$ decay of the density. In Sec. III we present numerical simulations of the reaction, focusing, in particular, on the density decay exponent, the domain length growth exponent, and the behavior of the scaled domain density profile. This latter consideration has previously been found to be fruitful in understanding both the kinetics and the spatial structure of reactants in $A+B\rightarrow 0$ with unbiased diffusion of each species [8]. The numerical results support many of our qualitative arguments. Finally, in Sec. IV we provide general conclusions as well as discuss the kinetics with arbitrary biases of each species and in higher spatial dimension.

II. ANALYTICAL APPROACHES

A. Single-species motion

Let us first recall some basic properties of single-species driven diffusion in one dimension where the positions of individual particles are updated sequentially and in random order [9]. Denote by $n_i(t)$ the occupation number for the ith site at time t. By the excluded-volume interaction, n_i is restricted to be either 0 or 1. Depending on the local configuration of particles on sites $i-1$, i, and $i+1$, the occupation number for site i at time $t+\delta t$ has three possible outcomes

$$n_i(t+\delta t)=\begin{cases} n_i(t) & \text{with probability } 1-2\alpha\delta t \\ n_i(t)n_{i+1}(t) & \text{with probability } \alpha\delta t \\ n_i(t)+[1-n_i(t)]n_{i-1}(t) & \\ \qquad \text{with probability } \alpha\delta t\ . & \end{cases} \tag{1}$$

Here δt is the microscopic time step and $\alpha\delta t$ is the probability that a particle attempts to move during the time step. These three possibilities have the following origins: If neither the ith nor the $(i-1)$th particles were selected for a move attempt, then $n_i(t)$ does not evolve, as indicated in the first line. The second line describes the state of site i at $t+\delta t$ if a move attempt is performed on the particle initially at site i. Similarly, the third line gives the state of site i if a move attempt is performed on a particle initially at site $i-1$.

Corresponding to these elemental updates, the Master equation for the average occupation number $\bar{n}_i(t)$ is

$$\bar{n}_i(t+\delta t)-\bar{n}_i(t)=\alpha\delta t[\bar{n}_i(t)\bar{n}_{i+1}(t)-\bar{n}_i(t)\bar{n}_{i-1}(t) +\bar{n}_{i-1}(t)-\bar{n}_i(t)]\ . \tag{2}$$

In writing this equation, we have exploited the fact that for one-dimensional driven diffusion in a finite ring or in an open system but sufficiently far from the boundaries, the occupation numbers for the different sites are uncorrelated [9]. This implies that a mean-field description is exact so that the two-particle correlation function $\overline{n_i(t)n_j(t)}$ may be replaced by the product of single-particle densities $\bar{n}_i(t)\bar{n}_j(t)$ in Eq. (2). In the continuum limit, the leading-order expansion of the above Master equation yields the Burgers equation

$$\frac{\partial\bar{n}}{\partial t}=-\frac{\Delta x}{\Delta t}\frac{\partial}{\partial x}[\bar{n}(1-\bar{n})]+\frac{\Delta x^2}{2\Delta t}\frac{\partial^2\bar{n}}{\partial x^2}\ , \tag{3}$$

where Δx is the lattice spacing and $\Delta t=\alpha^{-1}$ is a macroscopic time step during which one move attempt is performed, on average, for each particle. In this equation, terms of order $\Delta x^3/\Delta t$ and higher powers of Δx are neglected. In the following we choose the length and time scales such that $\Delta x=1$ and $\Delta t=1$.

This Burgers equation may be solved by first reducing it to the diffusion equation by a Cole-Hopf transformation [10]. Since the latter equation is trivially soluble, the solution to the Burgers equation may be obtained by performing an inverse Cole-Hopf transformation on the corresponding diffusive solution. A sketch of the Burgers equation solution in the long-time limit for a localized initial source $\bar{n}(x,0)=A\delta(x)$ is shown in Fig. 1. There are three universal regions in the long-time solution that are independent of the microscopic details of the initial density distribution. First, there is a constant-slope "interior" region where $\bar{n}(x,t)\approx(1-x/t)/2$, with x in the domain $t-2\sqrt{At}\le x\le t$. This behavior arises because the leading low-density particles have a relatively large velocity and continue to propagate faster than the denser trailing particles. At either end of this interior region, i.e., at $x=t-2\sqrt{At}$ and t, there are two diffusive boundary regions whose widths grow as $\sim\sqrt{t}$. In the interior region, the solution to Eq. (3) is asymptotically close to the profile of the solution of the inviscid Burgers equation (shown dotted in the figure). This inviscid solution consists of the line segment $\bar{n}_{\text{inviscid}}(x,t)=(1-x/t)/2$ for $t-2\sqrt{At}<x<t$, while $\bar{n}_{\text{inviscid}}(x,t)=0$ otherwise.

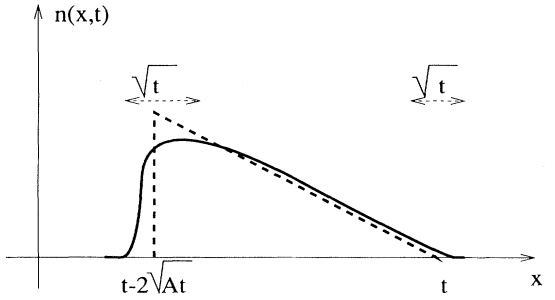

FIG. 1. Asymptotic solution of the Burgers equation for the initial value problem $n(x,t=0)=A\delta(x)$ with (——) and without (— — —) the viscosity term.

B. Dynamics of a single interface

To understand the evolution of domains in the initially homogeneous system it is helpful to determine the dynamics of a single AB interface. Therefore consider the "separated" initial condition where $n_A(x,t=0)=\bar{n}_A$ for $x<0$ and $n_A(x,t=0)=0$ for $x>0$, whereas $n_B(x,t=0)=0$ for $x<0$ and $n_B(x,t=0)=\bar{n}_B$ for $x>0$ (Fig. 2). The evolution of such a system provides essential insights into the nature of the reaction front [11–16] and has proven useful in understanding spatial structure in $A+B\rightarrow 0$ with homogeneous initial conditions, since relatively sharp reaction fronts naturally form as the system evolves. For the separated system, we will apply a mean-field approach in which the free motion of the A and B particles is modeled by the inviscid Burgers equa-

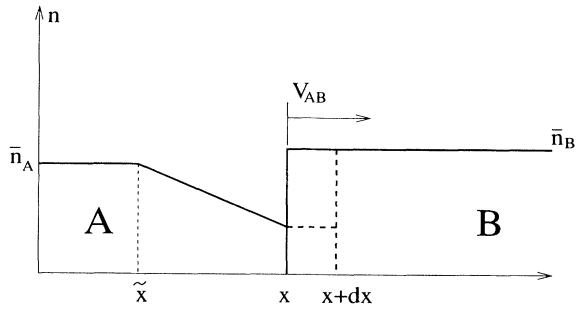

FIG. 2. Schematic illustration of evolution of the interface between two initially separated A and B domains. The motion of each species is described by the inviscid Burgers equation. There is a depletion zone in the A distribution that begins at $\tilde{x}$ and extends to the interface. In a time dt, the interface advances from x to $x+dx$ and the initially uniform B distribution in the slab $[x,x+dx]$ is replaced with a slowly varying A distribution whose density is approximately equal to the A density at the interface.

tion. Then by invoking mass balance at the AB interface, we determine the interface velocity and the spatial distribution of reactants.

Assume that the interface initially at $x=0$ moves from x to $x+dx$ in a time dt. Thus the B's within the slab $[x,x+dx]$ will be completely replaced by A's. Consequently, the incident flux of A, j_A, must be sufficient to annihilate all the B's that do not escape from the slab and also repopulate the slab at the final density of A's. That is,

$$j_A dt = n_A dx + R \ , \tag{4a}$$

where R represents the A's that will undergo reaction in the slab. Similarly, the outgoing flux of B, j_B, includes the initial number of B's in the slab minus those that disappear by reaction:

$$j_B dt = n_B dx - R \ . \tag{4b}$$

These two lead to the mass balance equation

$$[j_A(x,t)+j_B(x,t)]dt=[n_A(x,t)+n_B(x,t)]dx \ , \tag{5}$$

where $dx = v_{AB}dt$, with v_{AB} being the interface velocity. In the inviscid Burgers equation these currents are related to the corresponding particle densities n_A and n_B by

$$\begin{aligned} j_A(x,t)&=n_A(x,t)[1-n_A(x,t)] \ , \\ j_B(x,t)&=n_B(x,t)[1-n_B(x,t)] \ . \end{aligned} \tag{6}$$

The concentration of A at the interface depends upon whether the interface itself moves faster or slower than the point $\tilde{x}$ that defines the beginning of the depletion zone for the A distribution (Fig. 2). According to the Burgers equation, this boundary point moves with velocity $\tilde{v}=1-2\bar{n}_A$. Thus if the interface moves to the right faster than $\tilde{x}$, the hypothesized depletion zone exists and the concentration of A at the interface coincides with solution of the inviscid Burgers equation. On the other hand, if $v_{AB}<\tilde{v}$, the depletion zone does not appear and the concentration of A is constant throughout the domain. Thus for the concentration of A at the interface, we have

$$n_A(x,t)=\begin{cases} (1-x/t)/2 & \text{for } v_{AB}\geq\tilde{v} \\ \bar{n}_A & \text{otherwise} \ . \end{cases} \tag{7}$$

On the other hand, since the concentration of B remains constant throughout the domain

$$n_B(x,t)=\bar{n}_B \ . \tag{8}$$

Substituting Eqs. (6)–(8) and the relations $dx/dt=v_{AB}$ and $\tilde{v}=1-2\bar{n}_A$ into the mass balance equation (5) gives

$$v_{AB}=\begin{cases} 1-2\bar{n}_B(\sqrt{2}-1) & \text{for } \bar{n}_A\geq\bar{n}_B(\sqrt{2}-1) \\ 1-\dfrac{\bar{n}_A^{\,2}+\bar{n}_B^{\,2}}{\bar{n}_A+\bar{n}_B} & \text{for } \bar{n}_A<\bar{n}_B(\sqrt{2}-1) \ . \end{cases} \tag{9}$$

To check whether these formulas account for the propagation of an AB interface on a microscopic level, we numerically simulated the $A+B\rightarrow 0$ reaction with initially separated species that undergo the same driven diffusive motion. The agreement between the simulation data and the model predictions indicate that our phenomenological description based on mass balance and the inviscid Burgers equation accurately accounts for the microscopic behavior (Fig. 3). However, the actual width of the reaction zone is primarily controlled by diffusion and therefore its behavior is beyond the scope of an inviscid model.

C. Density decay and domain growth rates

Let us now return to the original problem of equal initial concentrations of A and B that are randomly distributed. As time increases, a region initially rich in a particular species (due to initial density fluctuations) will evolve into a single-species domain. To determine the time dependence of the size of such a domain, note that if the domain length is L, the initial excess of a particular species and thus the number of particles remaining within it after the minority species is annihilated is typically of order $\sqrt{L}$. Consequently, the concentration in a typical domain is of order [1–5]

$$n(t)\sim 1/\sqrt{L(t)} \ . \tag{10}$$

On the other hand, from Eq. (9) the rate of change of the domain length dL/dt is equal to the difference of the velocities of its two boundaries

$$dL/dt \propto |v_{AB}-v_{BA}| \ . \tag{11a}$$

Also from Eq. (9) this velocity difference is proportional to the density difference across the interfaces. These differences are typically of the order of the domain densities themselves. Thus we conclude that

$$dL/dt \sim n_A - n_B \sim n(t) \ . \tag{11b}$$

Combining Eqs. (10) and (11), we predict that the domain size grows as $L\sim t^{2/3}$, while the density decays as

$$n(t)\sim t^{-1/3} \ . \tag{12}$$

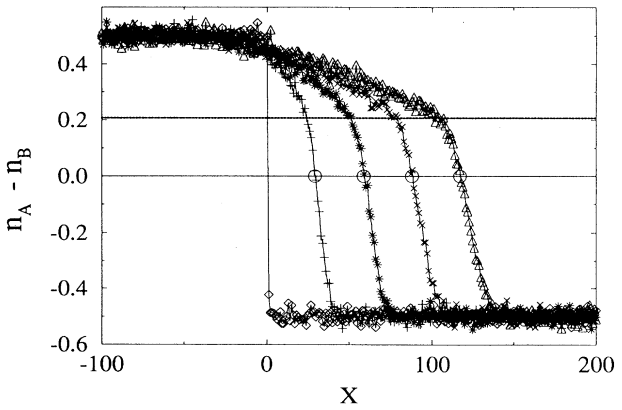

FIG. 3. Density profile near the AB interface at $t=0$ ($\diamond$), $t=50$ (+), $t=100$ ($*$), $t=150$ ($\times$), and $t=200$ ($\triangle$), for 300 configurations with $\bar{n}_A=\bar{n}_B=0.5$. The calculated positions of the interface are marked by $\circ$. The upper line shows the calculated value of $n_A=0.207$ for the A density at the interface.

It is also instructive to estimate the leading correction to this result. Recall that the difference between the solution of the inviscid and viscid Burgers equation occurs in the boundary regions whose widths are proportional to $\sim\sqrt{t}$ (Fig. 1). Consequently, the inclusion of a viscosity term should lead to a $t^{1/2}$ correction to the typical domain length, i.e., $L\sim At^{2/3}+Bt^{1/2}$. Correspondingly, this gives rise to a correction of order $\sim t^{-1/6}$ to the asymptotic behavior of the density. This slowly vanishing correction is a possible reason for slow convergence of the previous [6] and our simulations to the predicted asymptotic behavior.

III. SIMULATION RESULTS

We performed simulations on a system of 5×10^5 lattice sites of $1.5^{30}\cong 1.9\times 10^5$ time steps and averaged over 30 initial configurations. As has been observed previously [6], the local estimate of the density decay exponent from our data is systematically decreasing with time [Fig. 4(a)]. The abscissa $t^{-1/6}$ is used based on the expectation that asymptotic corrections will be of order $t^{-1/6}$, as discussed above. At long times, the initial density difference in each realization becomes an appreciable fraction of the density itself and departures from power-law scaling are anticipated. With these caveats, a limiting value of $-\frac{1}{3}$ for the density decay exponent is not incompatible with our data. A larger-scale simulation would help resolve this issue. Another basic quantity that also exhibits slow approach to asymptotic behavior is the average domain length $L(t)$ [Fig. 4(b)]. The local exponent of this quantity grows systematically with time and an asymptotic value $\frac{2}{3}$, which was predicted in our phenomenological approach, is again not incompatible with the data, subject to the above-mentioned caveats.

A deeper understanding of the behavior of the system can be gained by examining the distribution of particles within a domain. In the case of $A+B\rightarrow 0$ with isotropic diffusion, we examined both the "microcanonical" and "canonical" domain profiles [8]. To construct the former, we first define the extent of a particular domain of A, say, by the distance between the two B particles that enclose this A domain. We then rescale the lengths of individual domains to a constant value and then superpose the corresponding rescaled densities. Finally, it is convenient to plot the scaled profile $\rho(x/L,t)t^{1/3}$, where $\rho(x/L,t)$ is the local density within a domain at scaled position x/L and time t (see Fig. 5). These data collapse onto a universal curve, except for the leading and trailing regions, where the slopes for later time seem to be steepening. We suggest that the departure from scaling can be partially understood by recalling that the boundary layers around each domain grow as $\sqrt{t}$, while a domain by itself grows as $t^{2/3}$. Thus the relative width of the boundary layer decreases as $t^{-1/6}$, leading to the slope of the scaled density profile growing as $t^{1/6}$. To illustrate this effect, we plot, in Fig. 6, the trailing tail of the microcanonical domain profile when the ordinate is rescaled according to $t^{1/6}$. The apparent existence of scaling according to $t^{1/6}$ in this subregion suggests that there are really two length scales for a single domain.

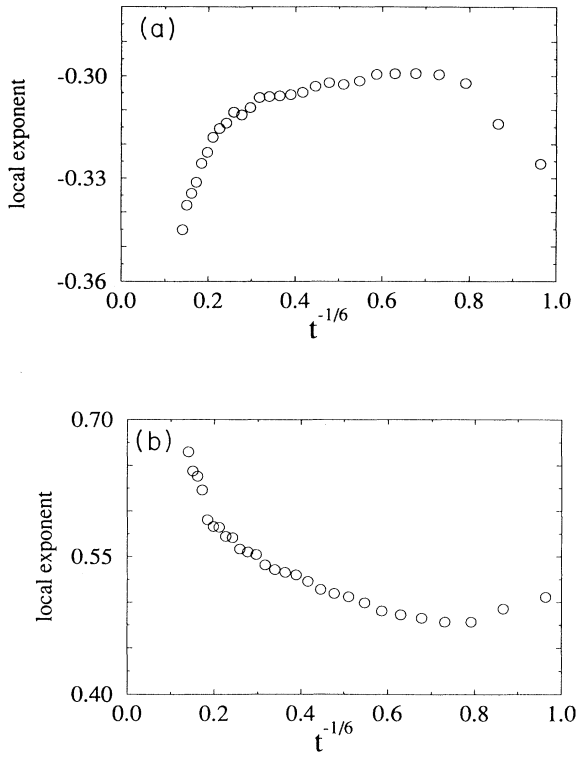

FIG. 4. Time dependence of the local exponents for (a) the density decay exponent and (b) the domain length exponent.

One, growing as $t^{2/3}$, corresponds to the "bulk" domain growth and is described by the inviscid Burgers equation. The other, corresponding to the boundary layer, grows as $\sim\sqrt{t}$ and may be described only by including the higher-order viscosity term in the Burgers equation.

We have also examined the canonical density profile in which the densities of all domains are superposed about a common center, but without rescaling the domains lengths before the superposition. Strikingly, these

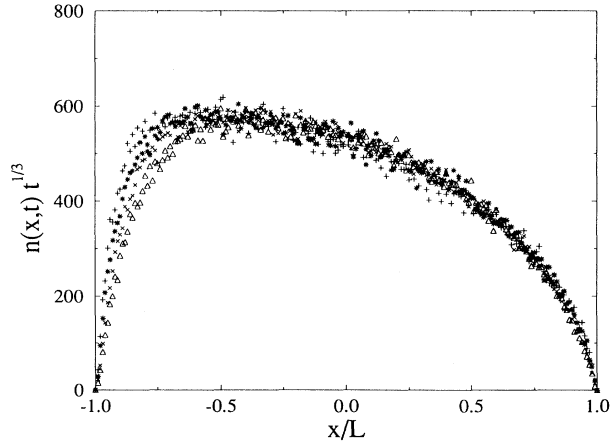

FIG. 5. Scaled microcanonical density profiles at $t=1.5^{18}\cong 1477$ (△), $t=1.5^{21}\cong 4987$ (×), $t=1.5^{24}\cong 16\,833$ (*), and $t=1.5^{27}\simeq 56\,814$ (+).

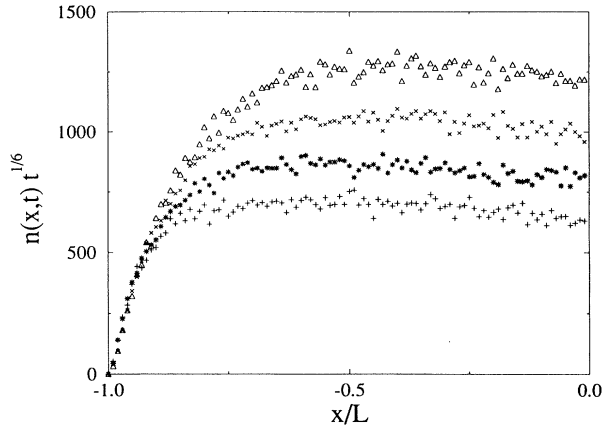

FIG. 6. Trailing edge of the microcanonical density profiles when rescaled by the factor $t^{1/6}$. The symbols refer to the same times as in Fig. 5.

profiles are nearly symmetric about a point that is centered a very small distance upstream from the domain center (Fig. 7). Furthermore, the decay of this profile is quite accurately described by a simple exponential.

IV. DISCUSSION

To summarize and to place our results in an appropriate context, it is helpful to consider the $A+B\to 0$ reaction when there are arbitrary hopping anisotropies β_A and β_B, respectively, for the A and B species. Thus, for a given species, the probability for a particle to jump to the right is $(1+\beta)/2$ and to the left is $(1-\beta)/2$. The model we have considered thus far corresponds to the extreme case of $\beta_A=\beta_B=1$, i.e., particles hop only to the right. The general case can be usefully described in terms of the "phase diagram" whose axes are the degree of anisotropy of each species (Fig. 8).

In the continuum limit, it straightforwardly follows

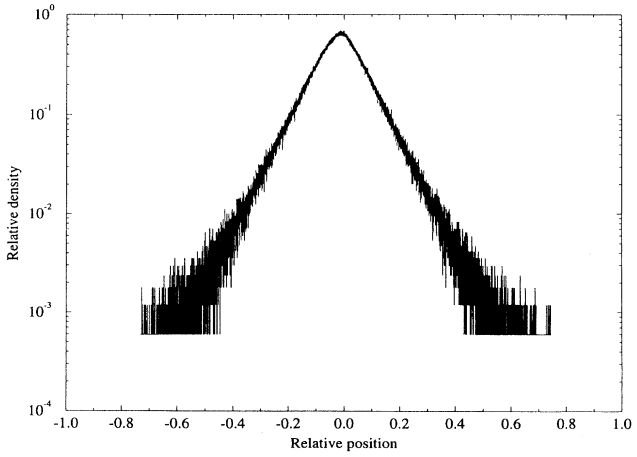

FIG. 7. Canonical density profile at $t=1.5^{21}\cong 4987$.

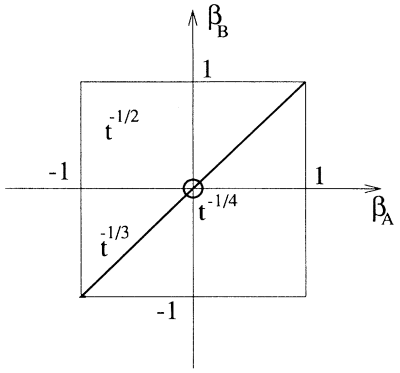

FIG. 8. "Phase diagram" for the density decay exponent for different hopping anisotropies of the A and B species.

that for arbitrary but equal biases of A and B $(0<\beta_A=\beta_B\equiv\bar{\beta}\leq 1)$, the Burgers equation, Eq. (3) will be modified only by the introduction of the coefficient $\bar{\beta}$, which multiplies the first-order spatial derivative

$$\frac{\partial\bar{n}}{\partial t}=-\bar{\beta}\frac{\partial}{\partial x}[\bar{n}(1-\bar{n})]+\frac{1}{2}\frac{\partial^2\bar{n}}{\partial x^2}\ . \tag{13}$$

Such a coefficient in the equation of motion can be absorbed by a suitable rescaling of x and t, leading to universal behavior in the hopping anisotropy, as long as this anisotropy is nonzero and the same for both species. Hence the density decay exponent along the line $\beta_A=\beta_B$ is expected to be equal to $-\frac{1}{3}$, except for $(\beta_A,\beta_B)=(0,0)$. This singular point corresponds to the case of pure diffusion where the density decay exponent equals $-\frac{1}{4}$, independently of the existence of a same species hard core repulsion [1–5,8].

The remainder of the phase diagram corresponds to systems with unequal biases for the two species. Applying the arguments of Sec. II, the evolution of the typical domain length is determined by the difference in the velocities at each interface. This gives $dL/dt\sim\beta_A-\beta_B$, so that the average domain size grows linearly in time. Consequently, the concentration varies as $n(t)\sim 1/\sqrt{L}\sim 1/\sqrt{t}$. Our simulations of $A+B\to 0$ with an unequal biases for A and B are consistent with this heuristic prediction.

Thus diffusion-controlled two-species annihilation with same-species hard-core repulsion has a rich variety of kinetic behaviors in one dimension. The decay exponent equals $\frac{1}{4}$, $\frac{1}{3}$, and $\frac{1}{2}$ for zero, equal, and unequal biases, respectively. For the first and third situations, rate equation approaches have failed to give the correct asymptotic behavior. In contrast, for the equal bias case we have shown that the Burgers equation approach, supplemented by mass balance at the interfaces between domains, explains several characteristics of the system. More subtle features, such as the density profile inside the domains, are beyond the simple-minded approach developed here, but might be accessible by a refinement of our technique. It is also worth mentioning that microscopic characteristics of the system, e.g., the typical domain size $L\sim t^{2/3}$,

naturally arise in other contexts where the Burgers equation plays the leading role [17].

Finally, it is worth considering the effect of driven motion on $A+B\rightarrow 0$ in greater than one spatial dimension. Numerically, we have investigated two natural versions: In the north-east model, we allow particles to move either up or to the right with equal probabilities, while in the north-east-south model, we allow particles to move up, down, or to the right with equal probabilities. For both cases, the density appears to decay asymptotically as $t^{-1/2}$. Interestingly, there is a significant time range where the density decay exponent is clearly less than $-\frac{1}{2}$. This same anomaly also appears in $A+B\rightarrow 0$ with isotropic diffusion of the reactants however. This can be ascribed to the existence of a limited temporal regime where there is some penetration of particles of one species into a domain of the opposite species. This effect is even more strongly pronounced in three dimensions [18].

Qualitatively, one can estimate the effect of driven diffusion on the reaction kinetics in arbitrary dimension d. If L is the typical length of a single-species domain in the drift direction, then its volume V scales as $Lt^{(d-1)/2}$ since the domain length in the remaining $d-1$ transverse directions still grows by diffusion. Repeating now the steps employed in the previous treatment of the one-dimensional situation, we have $dL/dt\sim n$ and $n\sim V^{-1/2}\sim L^{-1/2}t^{-(d-1)/4}$. These can be readily solved to yield

$$n\sim\begin{cases} t^{-(d+1)/6} & \text{for } d\leq 2 \\ t^{-d/4} & \text{for } 2<d\leq 4 \\ t^{-1} & \text{for } d>4\ . \end{cases} \tag{14}$$

Our simulations are covered by the first line of Eq. (14). When $d>2$, the longitudinal length predicted by the above argument, $L\sim t^{(5-d)/6}$, is smaller than the diffusional length scale. This indicates that the drift is irrelevant above two dimensions and the reaction kinetics is the same as two-species annihilation with isotropic diffusion.

Note added. As this paper was being written, we learned of parallel work by Janowsky [19]. Although the spirit of our approaches are compatible, there are some quantitative disagreements of our respective simulation results.

ACKNOWLEDGMENTS

We thank D. ben-Avraham, S. Esipov, and V. Privman for helpful discussions. We also gratefully acknowledge ARO Grant No. DAAH04-93-G-0021 for partial support of this research.

[1] Ya. B. Zel'dovich and A. A. Ovchinnikov, Chem. Phys. **28**, 215 (1978); Ya. B. Zel'dovich and A. S. Mikhailov, Usp. Fiz. Nauk **153**, 469 (1987) [Sov. Phys. Usp. **30**, 23 (1988)].

[2] D. Toussaint and F. Wilczek, J. Chem. Phys. **78**, 2642 (1983).

[3] K. Kang and S. Redner, Phys. Rev. Lett. **52**, 955 (1984); Phys. Rev. A **32**, 435 (1985).

[4] G. Zumofen, A. Blumen, and J. Klafter, J. Chem. Phys. **82**, 3198 (1985).

[5] M. Bramson and J. L. Lebowitz, J. Stat. Phys. **62**, 297 (1991); **65**, 941 (1991).

[6] S. A. Janowsky, Phys. Rev. E **51**, 1858 (1995).

[7] V. Privman, A. M. R. Cadilhe, and M. L. Glasser (unpublished).

[8] F. Leyvraz and S. Redner, Phys. Rev. A **46**, 3132 (1992); see also S. Redner and F. Leyvraz, in *Fractals and Disordered Systems, Vol. II,* edited by A. Bunde and S. Havlin (Springer-Verlag, Berlin, 1993).

[9] H. Spohn, *Large-Scale Dynamics of Interacting Particles* (Springer-Verlag, Berlin, 1991), Pt. II, Chaps. 4 and 5.

[10] G. B. Whitham, *Linear and Nonlinear Waves* (Wiley-Interscience, New York, 1974), Chap. 4.

[11] L. Gálfi and Z. Rácz, Phys. Rev. A **38**, 3151 (1988).

[12] H. Larralde, M. Araujo, S. Havlin, and H. E. Stanley, Phys. Rev. A **46**, 855 (1992); **46**, 6121 (1992).

[13] S. Cornell and M. Droz, Phys. Rev. Lett. **70**, 3824 (1993).

[14] E. Ben-Naim and S. Redner, J. Phys. A **25**, L575 (1992).

[15] B. Lee and J. Cardy, Phys. Rev. E **50**, 3287 (1994).

[16] P. L. Krapivsky, Phys. Rev. E **51**, 4774 (1995).

[17] T. Tatsumi and S. Kida, J. Fluid Mech. **55**, 659 (1972); S. F. Shandarin and Ya. B. Zel'dovich, Rev. Mod. Phys. **61**, 185 (1989).

[18] F. Leyvraz, J. Phys. A **25**, 3205 (1992).

[19] S. A. Janowsky, preceding paper, Phys. Rev. E **52**, 2535 (1995).